Identification of the tumor-suppressive role of circular RNA-FOXO3 in colorectal cancer via regulation of miR-543/LATS1 axis

YUN-YAO DENG[1*], YU-JUAN MIN[2*], KUN ZHOU[1*], QING-SONG YANG[3], MEI PENG[1], ZHAO-RUI CUI[4], XIANG-LIAN ZHU[4], HAO LIU[4], MIN WANG[5], XIE ZHANG[6] and LI-XIN LIU[1]

[1]Department of General Surgery, The Third Affiliated Hospital of Southern Medical University, Guangzhou, Guangdong 510630; [2]Department of General Surgery, The Second Clinical Medical College of North Sichuan Medical College, Nanchong, Sichuan 637000; [3]Department of General Surgery, Suzhou Sunset Care Institute, Suzhou, Jiangsu 215008; [4]Department of General Surgery, The First Affiliated Hospital of Jinan University, Guangzhou, Guangdong 510630; [5]Department of General Surgery, Women and Children's Hospital of Hunan, Changsha, Hunan 410008; [6]Department of General Surgery, Xiangtan Medicine and Health Vocational College, Xiangtan, Hunan 411104, P.R. China

Received December 12, 2019; Accepted July 31, 2020

DOI: 10.3892/or.2021.8190

Abstract. Colorectal cancer (CRC) is a common malignancy with significant prevalence and mortality rates. Circular RNA FOXO3 (circ-FOXO3; hsa_circ_0006404) has been reported to be involved in cancer regulation; however, its role in CRC is yet to be fully elucidated. Therefore, the aim of the present study was to investigate the effect of circ-FOXO3 on CRC progression and identify its underlying mechanism. In the present study, the expression of circ-FOXO3 was investigated in CRC tissues and cells via reverse transcription-quantitative PCR. A Cell Counting Kit-8 and colony formation assays were used to assess cell proliferation. The cell migratory and invasive abilities were detected using the Transwell migration and invasion assays. The luciferase assay and RNA pull-down assay were conducted to verify the relationship of circ-FOXO3, microRNA (miR)-543 and Large tumor suppressor kinase 1 (LATS1). The results demonstrated that circ-FOXO3 expression was downregulated in CRC tissues and cells, and was associated with poor overall survival of patients with CRC. Moreover, circ-FOXO3 was associated with tumor size, distant metastasis, differentiation, lymph node metastasis and TMN stages of patients with CRC. circ-FOXO3 overexpression suppressed CRC cell proliferation, migration and invasion. Luciferase assay and RNA pull-down assay results indicated that circ-FOXO3 functioned as a sponge for miR-543. In addition, circ-FOXO3 increased the expression of LATS1 via sponging miR-543, thus inhibiting CRC cell aggressive features. Collectively, the present results suggested that circ-FOXO3 inhibited CRC metastasis and progression via elevated LATS1 expression by sponging miR-543. Therefore, circ-FOXO3 may be a promising target for CRC therapy.

Correspondence to: Dr Xie Zhang, Department of General Surgery, Xiangtan Medicine and Health Vocational College, 6 Shuangyong Middle Road, Xiangtan, Hunan 411104, P.R. China
E-mail: yida520521@21cn.com

Dr Li-Xin Liu, Department of General Surgery, The Third Affiliated Hospital of Southern Medical University, 183 Zhongshan Avenue West, Tianhe, Guangzhou, Guangdong 510630, P.R. China
E-mail: kekoukele12389@139.com

*Contributed equally

Key words: circular RNA FOXO3, microRNA-543, large tumor suppressor kinase 1, colorectal cancer, migration, invasion

Introduction

Colorectal cancer (CRC) is a common malignancy associated with high prevalence and mortality rates (1,2). In 2018, 1.8 million new CRC cases were diagnosed worldwide (3). Mortality occurs in >600,000 patients with CRC annually (4), and thus CRC is considered a major cause of cancer-related mortality (5), as well as a serious threat to public health worldwide. Despite the substantial progress in early screening and therapeutic strategies, the survival of patients with CRC remains poor as a result of cancer metastasis. For instance, the 5-year survival rate of patients with CRC with distal metastasis is 12.5%, while it increases to ~90% in patients without metastasis (6,7). Therefore, it is important to identify the metastasis mechanism of CRC.

Circular RNAs (circRNAs), characterized by a closed-loop structure (8), are extensively expressed in human cells and serve post-transcriptional regulatory roles in genes expression (9). Moreover, numerous circRNAs contain microRNA (miRNA/miR) binding sites (10), and these circRNAs act as miRNA sponges (11) and regulate gene expression via

competing endogenous RNA (ceRNAs) mechanisms (12-14). circRNAs have been reported to participate in cancer progression. For example, circZNF609 acts as a miR-134-5p sponge to modulate B-cell translocation gene 2 expression, resulting in the repression of glioma cell proliferation and migration capacity (15). In addition, the elevated expression of circ-ASH2L in pancreatic cells and cancer tissues accelerates tumor progression via sponging miR-34a to upregulate Notch1 (16). At present, it has been revealed that circRNAs can regulate CRC cell aggressive features and cancer progression. For example, circ_0001178 promotes CRC progression and metastasis via sponging miR-382/587/616 (17). circ CBL.11 also inhibits CRC cell proliferation ability via regulating YWHAE by sponging miR-6778-5p (18).

As a vital circRNA, the regulatory action of circ-FOXO3 in cancer progression is an interesting research topic. For instance, Du *et al* (19) observed that circ-FOXO3 was decreased in tumor tissues, and overexpression of circ-FOXO3 resulted in tumor cell apoptosis. Moreover, circ-FOXO3 is downregulated in esophageal squamous cell cancer (ESCC) cells and tissues, and circ-FOXO3 overexpression restrains ESCC development by modulating miR-23a and PTEN (20). However, the effect of circ-FOXO3 on CRC remains unknown. Therefore, the aim of the present study was to investigate the role of circ-FOXO3 in CRC progression and identify the underlying mechanism.

Materials and methods

Patient section and cell culture. A total of 70 patients (age, 42-77 years; 24 males and 46 females) with CRC undergoing surgical resection between March 2017 and May 2018 in The Third Affiliated Hospital of Southern Medical University were enrolled in the current study. None of the patients underwent preoperative chemoradiotherapy. After all patients signed informed consent forms, the tumor tissues and healthy tissues adjacent to the tumor were collected and stored at -80˚C for subsequent experiments. The Ethics Committee of The Third Affiliated Hospital of Southern Medical University approved the study.

CRC cell lines, HT29 (cells were confirmed using short tandem repeat profiling), HCT116, HCT8, LOVO, SW480 and SW620, and wild-type colon epithelial cell line, FHC, were purchased from the American Type Culture Collection. HT29, HCT116, HCT8, LOVO, SW480 and SW620 cells were maintained in RPMI medium (Gibco; Thermo Fisher Scientific, Inc.) containing 10% FBS (Gibco; Thermo Fisher Scientific, Inc.) in a 37˚C incubator (Thermo Fisher Scientific, Inc.) with 5% CO_2. FHC cells were cultured in DMEM/F12 medium (Gibco; Thermo Fisher Scientific, Inc.) supplemented with 10% FBS, 10 mM HEPES, 5 μg/ml insulin, 10 ng/ml cholera toxin, 5 μg/ml transferrin and 100 ng/ml hydrocortisone (all Gibco; Thermo Fisher Scientific, Inc.) in a 37˚C incubator with 5% CO_2.

Reverse transcription-quantitative PCR (RT-qPCR). Total RNA was extracted from CRC tissues and cells using TRIzol® reagent (Sigma-Aldrich; Merck KGaA) and transcribed into the corresponding cDNA at 37˚C for 15 min followed by 10 sec at 85˚C using PrimeScript RT reagent kit with gDNA Eraser (Takara Biotechnology Co., Ltd.) and miR-X miRNA First-Strand Synthesis kit (Takara Biotechnology Co., Ltd.), according to the manufacturer's instructions. The qPCR reaction was conducted using SYBR Green PCR Master mix (Takara Biotechnology Co., Ltd.) and MiR-X miRNA RT-qPCR TB Green kit (Takara Biotechnology Co., Ltd.), according to the manufacturer's instructions. The PCR conditions were as follows: Initial denaturation at 95˚C for 5 min, followed by 40 cycles at 95˚C for 10 sec, 60˚C for 30 sec and 72˚C for 10 sec, and a final extension at 72˚C for 10 min. The sequences of primers were: circ-FOXO3 forward (F), 5'-GTG GGGAACTTCACTGGTGCTAAG-3' and reverse (R), 5'-GTCGTATCCAGTGCAGGGT-3' (21); miR-543 F, 5'-CTC CCTCCCGAATTTGAAG-3' and R, 5'-GTCAGAGGGAGA GGTCAG-3' (22); large tumor suppressor kinase 1 (LATS1) F, 5'-CCACCCTACCCAAAACATCTG-3' and R, 5'-CGC TGCTGATGAGATTTGAGTAC-3' (23); GAPDH F, 5'-CAT GAGAAGTATGACAACAGCCT-3' and R, 5'-AGTCCTTCC ACGATACCAAAGT-3' (21); and U6 F, 5'-GCGCGTCGTG AAGCGTTC-3' and R, 5'-GTGCAGGGTCCGAGGT-3' (22). GAPDH and U6 were used as internal references. The relative RNA expression was analyzed using the $2^{-\Delta\Delta Cq}$ method (24).

RNase R digestion assay. Total RNA was extracted using TRIzol® reagent (Sigma-Aldrich; Merck KGaA), and then 5 μg RNA was incubated with or without 3 U/μg RNase R (Epicentre Biotechnologies; Illumina, Inc.) at 37˚C for 15 min. The resulting RNA was purified using an RNeasy MinElute cleaning kit (Qiagen China Co., Ltd.) according to the manufacturer's instructions. Then, the expression levels of circ-FOXO3 and FOXO3 were determined using RT-qPCR assay. The primers of FOXO3 used in this study were: F, 5'-CGGCTA GCTGCGCCTTGGCTTTATAACT-3' and R, 5'-GGCTCG AGCCCTCCTTCACTGCTACTGG-3' (25).

Nuclear-cytoplasmic fractionation. HT29 and HCT116 cells ($1x10^7$) were lysed using cell fractionation buffer (Thermo Fisher Scientific, Inc.), followed by centrifuged at 16,000 x g for 5 min at 4˚C to separate nuclear and cytoplasmic fractions. The obtained nuclear and cytoplasm were used for extracting RNA using a PARIS kit (Thermo Fisher Scientific, Inc.), following the manufacturer's protocol. The extracted RNA was subjected to RT-qPCR to determine the expression of circ-FOXO3.

Cell transfection. The pcDNA circ-FOXO3, miR-543 mimic (5'-AAACAUUCGCGGUGCACUUCUU-3'), miR-543 inhibitor (5'-UACUUAAUGAGAAGUUGCCCGUGUUUU UUUCGCUUUAUUUGUGACGAAACAUUCGCGGUGCA CUUCUUUUUCAGUAU-3'), small interfering (si)-LATS1 (5'-GCAATCAGTTAACCGCAAA-3') and indicated controls, including pcDNA vector, miRNA mimic negative control (mimic NC) (5'-UUUGUACUACACAAAAGUACU G-3'), miRNA inhibitor NC (inhibitor NC) (5'-ACUACU GAGUGACAGUAGA-3'), siRNA NC (si-NC) (5'-GCACAG TTAACCGCATAAA-3') were obtained from Guangzhou RiboBio Co., Ltd. For cell transfection, cells ($1x10^6$) were inoculated into 6-well plates and maintained for 24 h at 37˚C, followed by transfection with 100 nM pcDNA circ-FOXO3, miR-543 mimic, miR-543 inhibitor or si-LATS1 using

Lipofectamine® 2000 (Invitrogen; Thermo Fisher Scientific, Inc.). After 48 h of transfection, HT29 and HCT116 cells were harvested for subsequent experiments. The transfection efficiency was determined using RT-qPCR and cell fluorescence.

For cell fluorescence, cells were fixed with 4% paraformaldehyde for 10 min at room temperature and incubated with Cy3-labeled miR-543 probe in hybridization buffer at 37˚C overnight. The nuclei were stained with DAPI for 5 min at room temperature. Cell fluorescence were captured under the confocal microscope at x40 magnification (Carl Zeiss AG).

Cell Counting Kit-8 (CCK-8) assay. HT29 and HCT116 cells were inoculated into 96-well plates ($1x10^3$ cells/well) and cultured at 37˚C. At indicated time points (0, 24, 48 and 72 h), HT29 and HCT116 cells in 96-well plates were further incubated with 10 μl CCK-8 reagent (Sigma-Aldrich; Merck KGaA) according to the manufacturer's instructions for 2 h at 37˚C. Cell viability was calculated based on the absorbance at 450 nm.

Colony formation assay. HT29 and HCT116 cells were made into a cell suspension and inoculated into 6-well plates (200 cells/well). After culturing for 14 days, HT29 and HCT116 cells were fixed using 4% paraformaldehyde (Sigma-Aldrich; Merck KGaA) for 15 min at room temperature and stained with 0.1% crystal violet (Sigma-Aldrich; Merck KGaA) for 15 min at room temperature. The number of colonies (>50 cells) was assessed manually.

Transwell migration and invasion assays. Transwell inserts with 8 μm pore size (Corning, Inc.) were inserted into 6-well plates. HT29 and HCT116 cells ($1x10^5$ cells/well) were inoculated into the upper chamber of Transwell and cultured in serum-free medium (Gibco; Thermo Fisher Scientific, Inc.). For cell invasion assays, the upper chamber of Transwell was covered with 50 μl Matrigel (BD Biosciences) at 37˚C for 2 h, which was the only difference to the migration assay. Complete medium supplemented with 10% FBS (Gibco; Thermo Fisher Scientific, Inc.) was added to the lower chamber of Transwell. After 24 h of cultivation, cells were fixed with 4% paraformaldehyde (Sigma-Aldrich; Merck KGaA) for 20 min at room temperature and stained with 0.1% crystal violet (Sigma-Aldrich; Merck KGaA) for 10 min at room temperature. The number of migrated and invaded cells was determined under a light microscope (Zeiss AG) in five random fields (magnification, x100).

Bioinformatics analysis. The circInteractome database (26) (https://circinteractome.nia.nih.gov/) was screened to identify miRNAs that were adsorbed by circ-FOXO3. miRanda (27) (http://www.microrna.org/) was used to search the target genes of miR-543.

Luciferase assay. The wild-type (WT) and mutant type (MUT) fragments of circ-FOXO3, and WT and MUT type 3'-untranslated region (3'-UTR) of LATS1 were synthesized and constructed into the pGL3 vector (Promega Corporation). Then, 100 nM circ-FOXO3 WT, circ-FOXO3 MUT, LATS1 WT 3'-UTR, LATS1 MUT 3'-UTR, miR-NC and miR-543 mimic were transfected into HT29 and HCT116 cells using Lipofectamine® 2000 (Thermo Fisher Scientific, Inc.). After 48 h of transfection, the luciferase activity was determined using a microplate reader (Thermo Fisher Scientific, Inc.) and normalized to *Renilla* luciferase activity.

RNA pull-down assay. Biotinylated-miR-543 probe and biotinylated NC (Bio-NC) probe were generated by Guangzhou RiboBio Co., Ltd. The RNA pull-down was performed as previously described (28). To produce probe-coated beads, miR-543 (Guangzhou RiboBio Co., Ltd.) was incubated with C-1 magnetic beads (Thermo Fisher Scientific, Inc.) for 2 h at 25˚C. The cell lysates were then harvested and treated with the 50 pmol miR-543 probe or Bio-NC probe overnight at 4˚C. After washing with wash/binding buffer, the RNA complexes adsorbed in the beads were collected and used to conduct RT-qPCR assay and northern blot analysis. For northern blot analysis, 30 μg RNAs were separated in a 1% agarose-formaldehyde gel and transferred to Hybond-N+ membrane (Beyotime Institute of Biotechnology). Then, the membranes were hybridized with digoxin-labeled DNA oligonucleotides specific to circ-FOXO3 (Guangzhou RiboBio Co., Ltd.) at 37˚C. The membranes were exposed to phosphorimager screens and analyzed using Image Lab V3.0 software (Bio-Rad Laboratories, Inc.).

Western blotting. Proteins were isolated from HT29 and HCT116 cells using RIPA buffer (Thermo Fisher Scientific, Inc.) and quantified using the BCA method. The extracted proteins (40 μg) were then separated on 10% SDS-PAGE and transferred to a PVDF membrane (Thermo Fisher Scientific, Inc.). After blocking with 4% skimmed milk for 1 h at room temperature, the membrane was probed with rabbit anti-human polyclonal LATS1 antibody (1:500; cat. no. ab70562), mouse anti-human monoclonal E-cadherin antibody (1:500; cat. no. ab76055), rabbit anti-human polyclonal N-cadherin antibody (1:500; cat. no. ab76057), rabbit anti-human polyclonal Vimentin antibody (1:500; cat. no. ab137321), mouse anti-human monoclonal MMP9 antibody (1:500; cat. no. ab119906) and rabbit anti-human polyclonal GAPDH antibody (1:1,000; cat. no. ab9485; all Abcam) at 4˚C for 12 h. After the washing steps, the membrane was incubated with HRP-conjugated rabbit polyclonal anti-human IgG H&L (1:1,000; cat. no. ab6759) or HRP-conjugated mouse monoclonal anti-human IgG H&L (1:1,000; cat. no. ab436; both Abcam) at room temperature for 1 h. GAPDH was used as the loading control. The blots were visualized using ECL western blotting substrate (Thermo Fisher Scientific, Inc.).

Statistical analysis. SPSS Statistics 22.0 (IBM Corp.) was utilized to conduct data analysis. Data are presented as the mean ± SD. Student's t-test or one-way ANOVA with Tukey's post hoc test were used for analyzing the significance between different groups. A paired t-test was used to compare the difference between tumor tissues and adjacent tissues. The relationship between circ-FOXO3 expression and the clinicopathological parameters of patients with CRC was determined using a χ^2 test. The overall survival of patients with CRC was determined using Kaplan-Meier analysis with the log-rank test. The correlations among the expression levels of circ-FOXO3, miR-543 and LATS1 were determined via correlation analysis

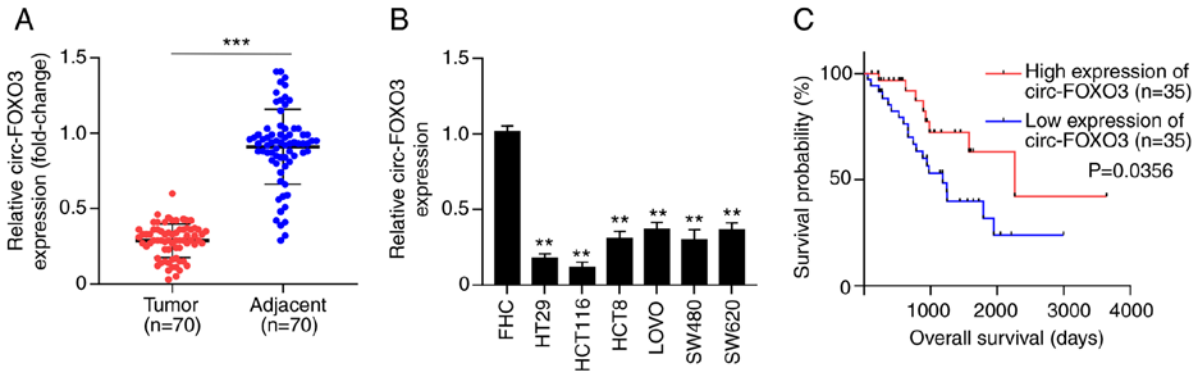

Figure 1. Expression of circ-FOXO3 in CRC tissues and cells. (A) Expression of circ-FOXO3 in tumor tissues and adjacent healthy tissues of 70 patients with CRC was determined via RT-qPCR. ***P<0.001. (B) Expression of circ-FOXO3 in CRC cells and human wild-type colon epithelial cell line was detected using RT-qPCR. **P<0.01 vs. FHC cells. (C) Kaplan-Meier analysis was used for analyzing the association between circ-FOXO3 expression and overall survival of patients with CRC. All experiments were performed three times. circ-FOXO3, circular RNA FOXO3; RT-qPCR, reverse transcription-quantitative PCR; CRC, colorectal cancer.

with a Pearson test. All experiments were repeated at least three times. P<0.05 was considered to indicate a statistically significant difference.

Results

circ-FOXO3 is downregulated in CRC tissues and cells. To assess the effects of circ-FOXO3 on CRC, the aberrant expression of circ-FOXO3 in CRC tissues was investigated. A significant downregulation of circ-FOXO3 expression was identified in tumor tissues compared with healthy tissues of 70 patients with CRC (P<0.001; Fig. 1A). In addition, circ-FOXO3 expression in CRC cells, including HT29, HCT116, HCT8, LOVO, SW480 and SW620, was significantly lower compared with wild-type colon epithelial cell line (all P<0.01; Fig. 1B).

To determine the association between circ-FOXO3 and clinical characteristics of patients with CRC, 70 patients with CRC were divided into the circ-FOXO3 high expression group and circ-FOXO3 low expression group based on the median value of circ-FOXO3 expression in CRC tissues as the cut-off value. Kaplan-Meier analysis demonstrated that the low expression of circ-FOXO3 was positively associated with poor overall survival of patients with CRC (P=0.0356; Fig. 1C). In addition, circ-FOXO3 expression was significantly associated with tumor size (P<0.01), distant metastasis (P=0.0003), differentiation (P=0.0002), lymph node metastasis (P<0.0001) and TMN stages (P=0.0081) (Table I). Therefore, these results suggested that circ-FOXO3 was downregulated in CRC, and associated with the overall survival, tumor size, distant metastasis, differentiation, lymph node metastasis and TMN stages of patients with CRC.

Overexpression of circ-FOXO3 suppresses CRC cell proliferation, migration and invasion. To investigate the effect of circ-FOXO3 on CRC, the role of circ-FOXO3 in CRC cell features was determined. It was identified that HT29 and HCT116 cells presented the lowest circ-FOXO3 expression compared with that in HCT8, LOVO, SW480 and SW620 cells (Fig. 1B). Thus, HT29 and HCT116 cells were used for follow-up experiments. First, a RNase R digestion assay was conducted in HT29 and HCT116 cells to assess the circular characteristics of circ-FOXO3. circ-FOXO3 was resistant to RNase R digestion, which indicated that circ-FOXO3 was a circRNA (P>0.05; Fig. 2A).

Subsequently, HT29 and HCT116 cells were transfected with pcDNA circ-FOXO3 plasmid to overexpress circ-FOXO3 expression, which were evaluated using RT-qPCR (P<0.0001 and P<0.001; Fig. 2B). The effect of circ-FOXO3 overexpression on CRC cell aggressive features was investigated after circ-FOXO3 overexpression. circ-FOXO3 overexpression significantly suppressed the viability of HT29 and HCT116 cells (all P<0.0001; Fig. 2C). Colony formation results indicated that the colony numbers of HT29 and HCT116 cells were significantly reduced after overexpression of circ-FOXO3 (all P<0.001; Fig. 2D). In addition, Transwell assays results found that circ-FOXO3 overexpression significantly inhibited cell migratory and invasive abilities (all P<0.0001; Fig. 2E and F). circ-FOXO3 overexpression also markedly increased the expression of E-cadherin, and notably decreased the expression levels of N-cadherin, Vimentin and MMP9 (Fig. 2G). Thus, these findings indicated that overexpression of circ-FOXO3 suppressed CRC cell proliferation, migration and invasion.

circ-FOXO3 functions as a miR-543 sponge. According to the aforementioned results, circ-FOXO3 presented aberrant expression in CRC and inhibited CRC cell aggressive features, but the underlying mechanism of their action remains to be determined. To identify the regulatory mechanism of circ-FOXO3 on CRC cell features, the location of circ-FOXO3 in CRC cells was first examined. A significantly higher expression of circ-FOXO3 was found in the cytoplasm compared with the nucleus of HT29 and HCT116 cells (all P<0.0001; Fig. 3A), which suggested that circ-FOXO3 was mostly located in the cytoplasm. circRNA in cytoplasm usually functions as a miRNA sponge (29). Therefore, it was hypothesized that circ-FOXO3 may function as a miRNA sponge in CRC cells to regulated CRC cell aggressive features.

The circInteractome database (https://circinteractome.nia.nih.gov/) was screened to identify miRNAs that are adsorbed by circ-FOXO3. A miR-543 binding site was found in circ-FOXO3, and the predicted sequences of circ-FOXO3 and miR-543 are presented in Fig. 3B. The transfection efficiency of miR-543 mimic was demonstrated using RT-qPCR

Table I. Association between circ-FOXO3 expression and clinicopathological parameters of patients with CRC.

Clinicopathological characteristics	Total	High expression	Low expression	χ^2	P-value
Sex					
Male	24	11	13	0.06341	0.8012
Female	46	24	22		
Age, years					
≤60	37	20	17	0.2293	0.632
>60	33	15	18		
Tumor size					
T1	17	14	3	16.33	0.001
T2	15	10	5		
T3	16	6	10		
T4	22	5	17		
Distant metastasis					
Positive	33	13	20	12.87	0.0003
Negative	37	22	15		
Differentiation					
High	26	6	20	17.37	0.0002
Moderate	21	10	11		
Poor	23	19	4		
Lymph node metastasis					
Positive	38	6	26	20.78	<0.0001
Negative	32	29	9		
TNM stages					
I	19	15	4	11.8	0.0081
II	14	8	6		
III	15	6	9		
IV	22	6	16		

Data were analyzed using a χ^2 test.

(all P<0.0001; Fig. S1A). Luciferase assay results demonstrated that miR-543 overexpression inhibited the relative luciferase activity in cells transfected with WT circ-FOXO3 (all P<0.001), while no significant effect was found in cells transfected with MUT circ-FOXO3 (Fig. 3B). RNA pull-down results indicated a significantly higher level of enrichment of circ-FOXO3 using the biotinylated-miR-543 probe compared with biotinylated-NC group in HT29 and HCT116 cells (all P<0.01; Fig. 3C). Moreover, overexpression of circ-FOXO3 decreased miR-543 expression (all P<0.001; Fig. 3D).

To further examine the association between miR-543 and circ-FOXO3, miR-543 expression in patients with CRC was detected, and it was found that miR-543 expression in tumor tissues was significantly upregulated compared with healthy tissues (P<0.0001; Fig. 3E). Pearson correlation analysis demonstrated a moderate negative correlation between the expression levels of miR-543 and circ-FOXO3 in CRC (P<0.0001; R=-0.5955; Fig. 3F). Thus, circ-FOXO3 may function as a miR-543 sponge.

circ-FOXO3 elevates LATS1 expression via sponging miR-543. Next, miR-543 targets were screened using miRanda (http://www.microrna.org/). LATS1 was considered as a potential target of miR-543 and the putative binding site sequences are presented in Fig. 4A. Luciferase assay was conducted to identify whether miR-543 targeted LATS1. It was found that miR-543 overexpression suppressed relative luciferase activity in cells transfected with WT LATS1 (all P<0.001), while no significant effect was observed in cells transfected with mutant type LATS1 (Fig. 4A).

The transfection efficiency of miR-543 mimic and inhibitor in HT29 and HCT116 cells were determined via cell fluorescence, which indicated that the miR-543 mimic notably increased miR-543 expression, while miR-543 inhibitor decreased miR-543 expression (Fig. 4B). In addition, the transfection efficiency of the miR-543 inhibitor was verified using RT-qPCR (all P<0.001; Fig. S1B). The miR-543 inhibitor elevated the mRNA expression of LATS1 in HT29 (P<0.001) and HCT116 (P<0.001) cells, while miR-543 mimic inhibited the mRNA expression of LATS1 in HT29 (P<0.001) and HCT116 (P<0.01) cells (Fig. 4C). Similarly, the protein expression of LATS1 oppositely modulated by miR-543 (Fig. 4D). The miR-543 mimic decreased circ-FOXO3 mRNA expression (all P<0.01), while miR-543 inhibitor significantly

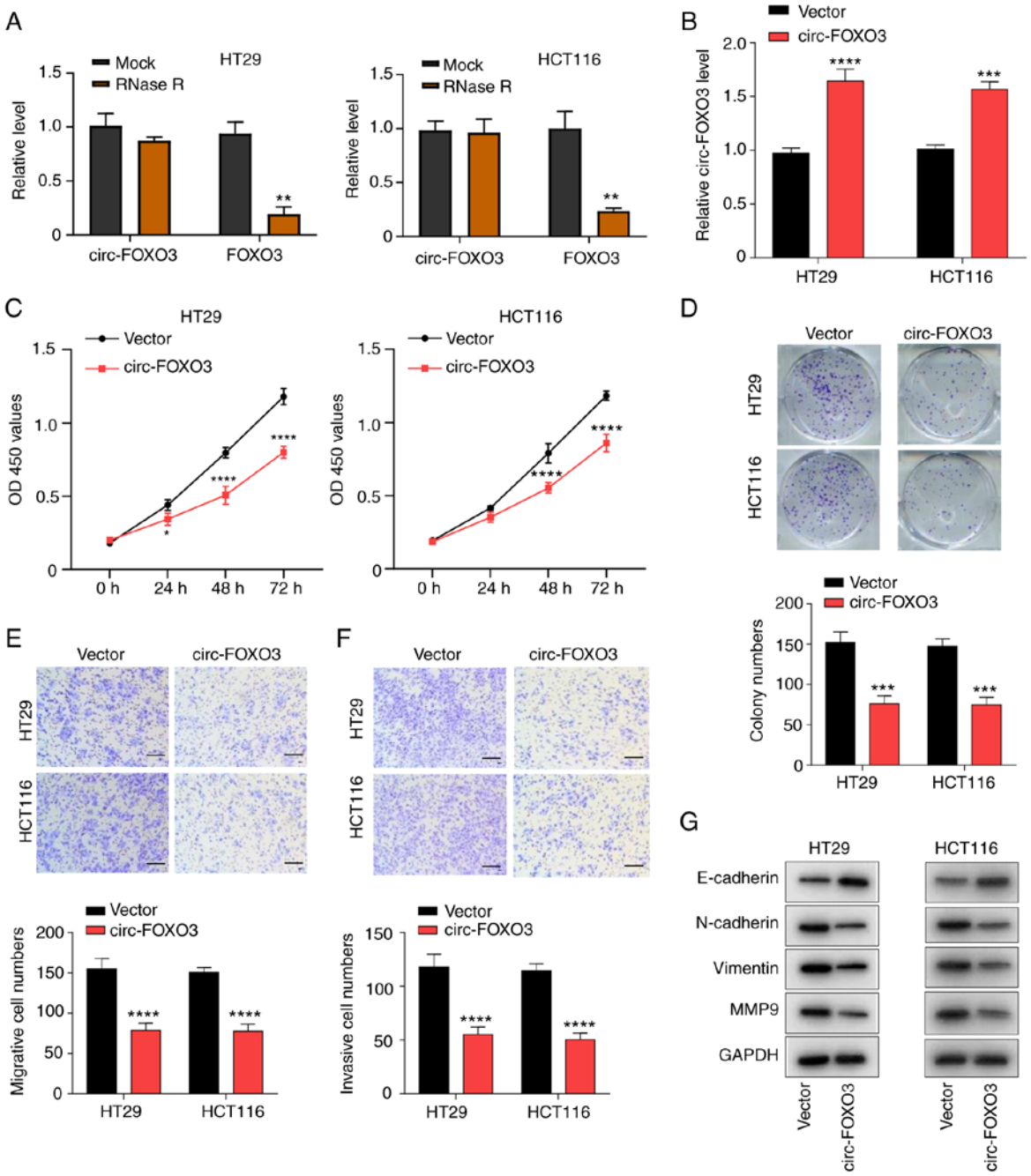

Figure 2. Overexpression of circ-FOXO3 inhibits colorectal cancer cell proliferation, migration and invasion. (A) Circular characteristic of circ-FOXO3 was assessed using RNase R digestion assay. (B) Reverse transcription-quantitative PCR was used to detect the transfection efficiency of pcDNA circ-FOXO3 in HT29 and HCT116 cells. (C) Cell Counting Kit-8 assay measured the viability of HT29 and HCT116 cells after circ-FOXO3 overexpression. (D) Colony formation assay determined the colony formation ability of HT29 and HCT116 cells after overexpression of circ-FOXO3. Transwell migration assay detected the (E) migratory and (F) invasive abilities of cells after overexpression of circ-FOXO3. Magnification, x100; Scale bar, 100 μm. (G) Western blotting was conducted to detect the protein expression levels of E-cadherin, N-cadherin, Vimentin and MMP9 in HT29 and HCT116 cells after overexpression of circ-FOXO3. All experiments were performed three times. *P<0.05, **P<0.01, ***P<0.001, ****P<0.0001 vs. Vector group. circ-FOXO3, circular RNA FOXO3; OD, optical density.

increased the expression of circ-FOXO3 (P<0.01 and P<0.001; Fig. 4E). Furthermore, the inhibitory effect of miR-543 mimic on LATS1 was reversed by circ-FOXO3 overexpression in HT29 and HCT116 cells (all P<0.01; Fig. 4F).

To further evaluate the association between LATS1 and circ-FOXO3, the expression of LATS1 was detected in patients with CRC, and it was identified that LATS1 was significantly downregulated in CRC tumor tissues compared with healthy tissues (P<0.0001; Fig. 4G). In addition, Pearson correlation analysis demonstrated a weak positive correlation between the expression levels of circ-FOXO3 and LATS1 (P<0.0001; R=0.3239; Fig. 4H). Collectively, these results suggested that circ-FOXO3 increased LATS1 expression via sponging miR-543.

miR-543 overexpression or LATS1 knockdown inhibits circ-FOXO3-induced attenuated CRC aggressive features. Based on the aforementioned results, it was suggested that the effect of circ-FOXO3 on CRC aggressive features may be mediated via miR-543 and LATS1. The transfection efficiency of si-LATS1

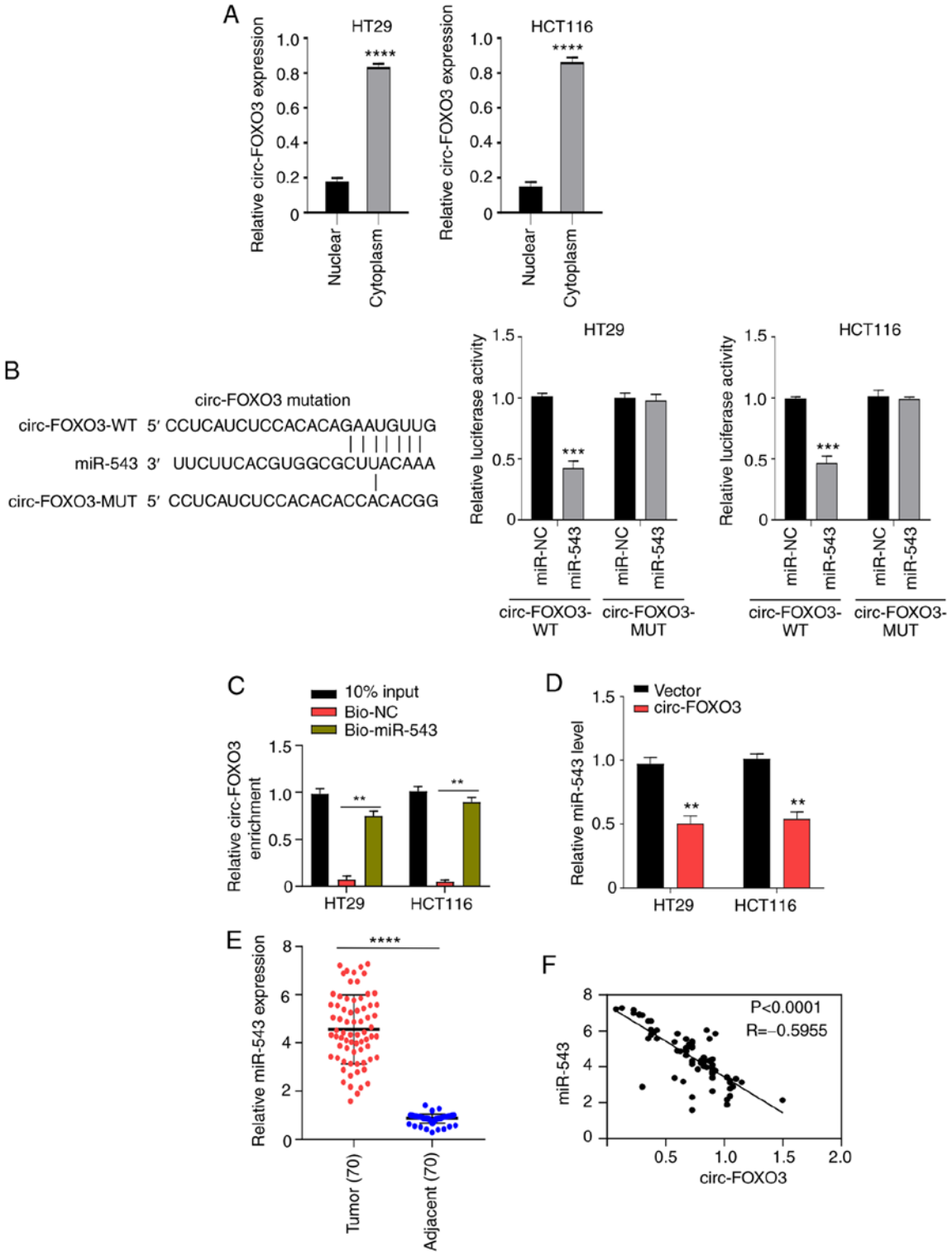

Figure 3. circ-FOXO3 acts as a sponge for miR-543. (A) Expression of circ-FOXO3 in nucleus and cytoplasm of HT29 and HCT116 cells was determined using RT-qPCR. ****P<0.0001 vs. Nuclear group. (B) Luciferase assay was performed to assess whether circ-FOXO3 directly binds to miR-543 in HT29 and HCT116 cells. ***P<0.001 vs. miR-NC group. (C) RNA pull-down was conducted to measure the enrichment of miR-543 using Bio-circ-FOXO3 in HT29 and HCT116 cells. **P<0.01 vs. Bio-NC group. (D) miR-543 expression was analyzed via RT-qPCR after overexpression of circ-FOXO3 in HT29 and HCT116 cells. **P<0.01 vs. Vector group. (E) Expression of miR-543 in tumor tissues and adjacent healthy tissues of 70 patients with colorectal cancer was determined using RT-qPCR. (F) Pearson correlation analysis determined correlation between the expression levels of miR-543 and circ-FOXO3. ****P<0.0001 vs. Adjacent group. All experiments were performed three times. circ-FOXO3, circular RNA FOXO3; RT-qPCR, reverse transcription-quantitative PCR; miR, microRNA; WT, wild-type; MUT, mutant; NC, negative control; Bio, biotinylated.

was verified using RT-qPCR (all P<0.001; Fig. S1C). The inhibitory role of circ-FOXO3 overexpression on cell viability was abolished by both miR-543 overexpression and LATS1 knockdown in HT29 and HCT116 cells (all P<0.001; Fig. 5A). Colony formation assay results demonstrated that both miR-543 overexpression (all P<0.01) and LATS1 knockdown (P<0.01

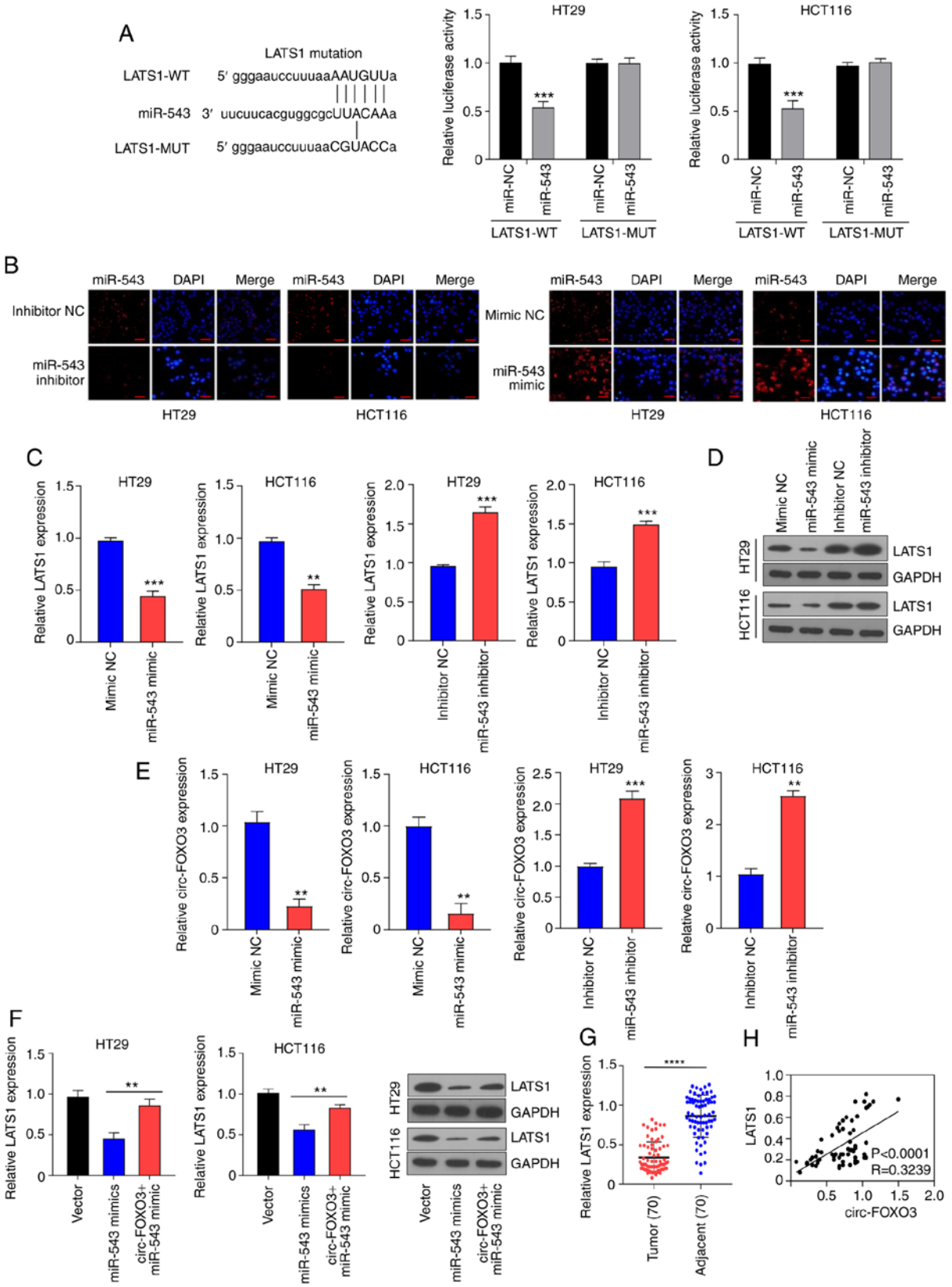

Figure 4. circ-FOXO3 increases LATS1 expression via sponging miR-543. (A) Luciferase assay was conducted to verify whether miR-543 directly binds to LATS1 in HT29 and HCT116 cells. (B) Transfection efficiency of miR-543 mimic and inhibitor in HT29 and HCT116 cells was determined using cell fluorescence. Magnification, x400; Scale bar, 50 μm. (C) mRNA and (D) protein expression levels of LATS1 in cells transfected with miR-543 mimic or inhibitor was determined using RT-qPCR and western blotting, respectively. (E) Expression of circ-FOXO3 in HT29 and HCT116 cells transfected with miR-543 mimic or inhibitor was determined using RT-qPCR. (F) mRNA and protein expression levels of LATS1 in cells transfected with pcDNA circ-FOXO3 or co-transfected with pcDNA circ-FOXO3 and miR-543 mimic in HT29 and HCT116. (G) RT-qPCR assay examined the mRNA expression of LATS1 in tumor tissues and adjacent healthy tissues of 70 patients with CRC. (H) Pearson correlation analysis determined the correlation between the expression levels of LATS1 and circ-FOXO3. All experiments were performed three times. **P<0.01, ***P<0.001, ****P<0.0001 vs. miR-NC group. circ-FOXO3, circular RNA FOXO3; RT-qPCR, reverse transcription-quantitative PCR; miR, microRNA; NC, negative control; WT, wild-type; MUT, mutant; LATS1, Large tumor suppressor kinase 1.

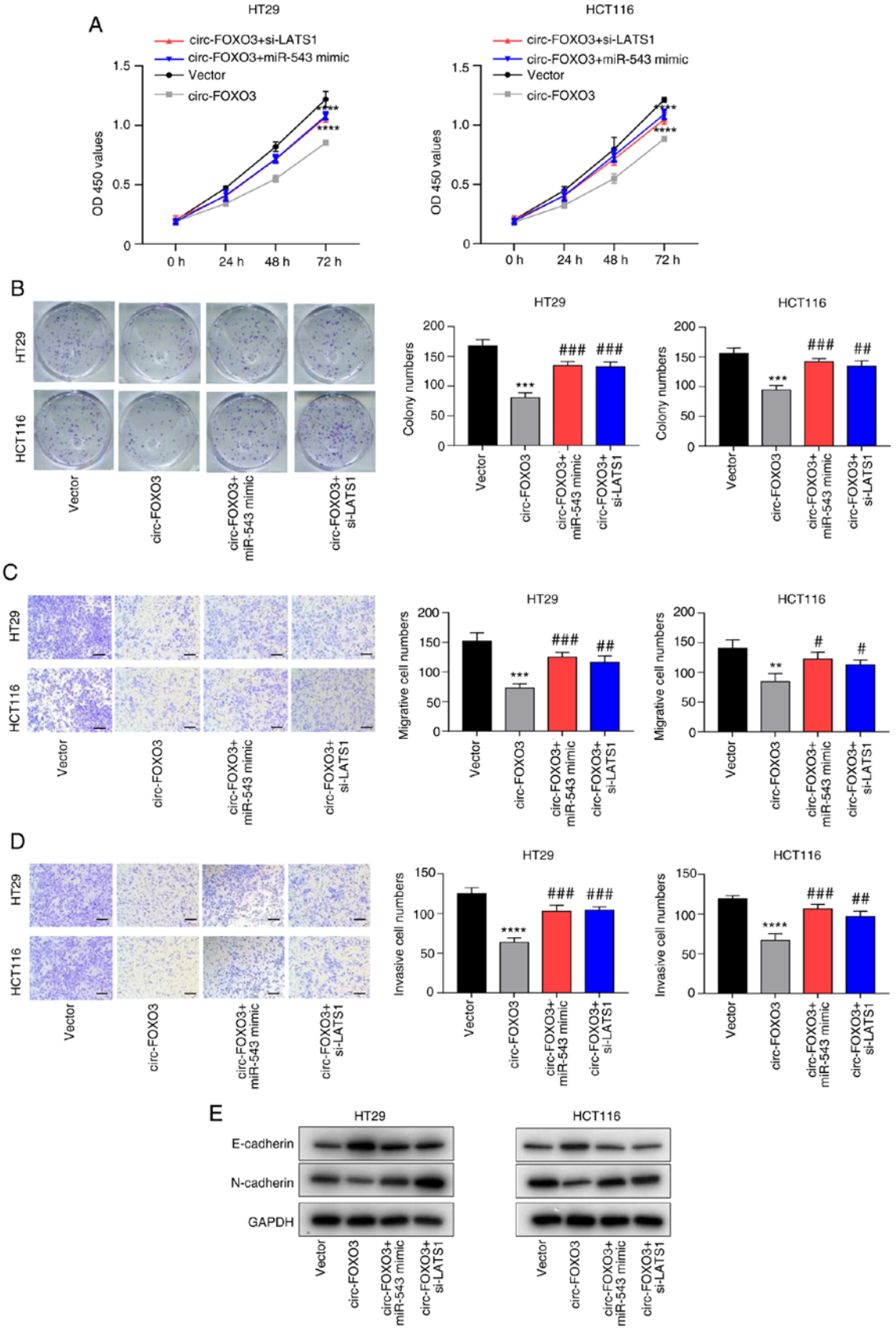

Figure 5. miR-543 overexpression or LATS1 knockdown blocks circ-FOXO3-induced attenuated CRC aggressive features. (A) Cell Counting Kit-8 assay was conducted to determine the viability of HT29 and HCT116 cells after the transfection of pcDNA circ-FOXO3, miR-543 mimic or si-LATS1. (B) Colony formation assay determined the colony formation ability of cells after the transfection of pcDNA circ-FOXO3, miR-543 mimic or si-LATS1. Transwell migration assay was conducted to assess the (C) migratory and (D) invasive abilities of HT29 and HCT116 cells after the transfection of pcDNA circ-FOXO3, miR-543 mimic or si-LATS1. Magnification, x100; Scale bar, 100 μm. (E) Western blotting was performed to detect the protein expression levels of E-cadherin and N-cadherin in cells after transfection of pcDNA circ-FOXO3, miR-543 mimic or si-LATS1. All experiments were performed three times. **P<0.01, ***P<0.001, ****P<0.0001 vs. Vector group; $^{\#}$P<0.05, $^{\#\#}$P<0.01, $^{\#\#\#}$P<0.0001 vs. circ-FOXO3 group. circ-FOXO3, circular RNA FOXO3; LATS1, Large tumor suppressor kinase 1; miR, microRNA; siRNA, small interfering RNA; OD, optical density.

and P<0.05) reversed the inhibitory effect of circ-FOXO3 overexpression on colony formation ability in HT29 and HCT116 cells (Fig. 5B). Furthermore, Transwell assay results identified that the inhibited migratory and invasive abilities exerted by circ-FOXO3 overexpression were blocked by miR-543 overexpression (P<0.05-P<0.001) or LATS1 knockdown (P<0.01 and P<0.05) in HT29 and HCT116 cells (Fig. 5C and D). The promotion effect of circ-FOXO3 overexpression on E-cadherin expression, and its inhibitory effects on N-cadherin expression were also markedly reversed by miR-543 overexpression or LATS1 knockdown in HT29 and HCT116 cells (Fig. 5E). Therefore, these results indicated that both miR-543 overexpression and LATS1 knockdown inhibited circ-FOXO3-induced attenuated CRC aggressive features.

Discussion

As a common malignancy, the morbidity and mortality rates of patients with CRC remain high despite the progress of early screening and therapeutic strategies (1,2). In 2018, 1.8 million new CRC cases were diagnosed worldwide (3). Mortality occurs in >600,000 patients with CRC annually, worldwide (4). The metastasis of cancer contributes to poor survival of patients with CRC (6,7). Hence, it is important to identify the metastasis mechanism of CRC. Recently, a previous study revealed that circRNAs participated in cancer metastasis regulation (30).

The present study investigated the effect of circ-FOXO3 on CRC progression. circ-FOXO3 expression was downregulated in CRC tissues and cells, which was in accordance with previous studies (19,20). Du *et al* (19) reported that circ-FOXO3 was reduced in tumor tissues of patients and cancer cells, while Xing *et al* (20) revealed decreased circ-FOXO3 expression in ESCC. Moreover, downregulation of circ-FOXO3 was associated with poor overall survival of patients with CRC, and was also found to be associated with tumor size, distant metastasis, differentiation, lymph node metastasis and TMN stages of patients with CRC. In line with these findings, Zhou *et al* (31) observed that circ-FOXO3 expression was downregulated in patients with *de novo* acute myeloid leukemia, and patients with low-expression of circ-FOXO3 had poor overall survival. Furthermore, the present results indicated that circ-FOXO3 overexpression suppressed CRC cell proliferation, migration and invasion *in vitro*, which were consistent with previous studies (19,20). For instance, in ESCC, elevated circ-FOXO3 was found to inhibit cell proliferation, migration and invasion (20).

circRNAs are generally involved in cancer progression by acting as miRNA sponges (11). For example, circ-FOXO3 could act as a miR-23a sponge in ESCC (20). In the current study, circ-FOXO3 was demonstrated to be a miR-543 sponge and could negatively regulate the expression of miR-543. miR-543 is a critical modulator in cancer progression (32-35), and it can accelerated esophageal cancer metastasis by directly binding to Phospholipase A2 Group IVA (32). miR-543 also promotes gastric cancer migration and invasion ability by targeting speckle type BTB/POZ protein (35).

miRNAs usually modulate cancer progression via binding to the target genes (36). Based on the present results, LATS1 was suggested to be a target of miR-543. LATS1 is a member of the LATS family and it acts as a tumor suppressor in different cancer types, such as gastric cancer and breast cancer (37,38). Moreover, LATS1 suppresses cancer cell proliferative and invasive abilities (39). circRNAs have been revealed to serve as miRNA sponges and modulate gene expression via ceRNA mechanisms (11). To determine whether circ-FOXO3 regulated gene expression via the ceRNAs mechanism, the relationship among circ-FOXO3, miR-543 and LATS1 was detected. The present results suggested that circ-FOXO3 elevated LATS1 expression via sponging miR-543. Furthermore, both miR-543 overexpression and LATS1 knockdown blocked circ-FOXO3-induced attenuated CRC aggressive cellular features. Thus, these findings indicated that overexpression of circ-FOXO3 inhibited CRC progression via elevated LATS1 expression by sponging miR-543. While the current study demonstrated the role and mechanism of circ-FOXO3 FoxO3 in CRC, a limitation of this study was the lack of *in vivo* experiments. Therefore, *in vivo* experiments will be conducted in a future study.

Collectively, the present study demonstrated that circ-FOXO3 expression was downregulated in CRC, and its overexpression inhibited CRC metastasis and progression via elevated LATS1 by sponging miR-543. Thus, circ-FOXO3 may be a promising target for CRC therapy.

Acknowledgements

Not applicable.

Funding

No funding was received.

Availability of data and materials

The datasets used and/or analyzed during the current study are available from the corresponding author on reasonable request.

Authors' contributions

YYD, YJM, KZ, XLZ and LXL designed the experiment. YYD, YJM and KZ wrote the manuscript. QSY, MP, ZRC acquired the data. LXL, HL, MW analyzed the data. XLZ and LXL approved the manuscript. YYD and LXL are responsible for confirming the authenticity of the raw data. All authors read and approved the final manuscript.

Ethics approval and consent to participate

After all patients signed informed consent forms, the tumor tissues and healthy tissues adjacent to the tumor were collected for subsequent experiments. The Ethics Committee of The Third Affiliated Hospital of Southern Medical University approved the study.

Patient consent for publication

Not applicable.

Competing interests

The authors declare that they have no competing interests.

References

1. Kemper KE, Glaze BL, Eastman CL, Waldron RC, Hoover S, Flagg T, Tangka FKL and Subramanian S: Effectiveness and cost of multilayered colorectal cancer screening promotion interventions at federally qualified health centers in Washington State. Cancer 124: 4121-4129, 2018.
2. Bray F, Ferlay J, Soerjomataram I, Siegel RL, Torre LA and Jemal A: Global cancer statistics 2018: GLOBOCAN estimates of incidence and mortality worldwide for 36 cancers in 185 countries. CA Cancer J Clin 68: 394-424, 2018.
3. Rawla P, Sunkara T and Barsouk A: Epidemiology of colorectal cancer: Incidence, mortality, survival, and risk factors. Prz Gastroenterol 14: 89-103, 2019.
4. Han P, Li JW, Zhang BM, Lv JC, Li YM, Gu XY, Yu ZW, Jia YH, Bai XF, Li L, *et al*: The lncRNA CRNDE promotes colorectal cancer cell proliferation and chemoresistance via miR-181a-5p-mediated regulation of Wnt/β-catenin signaling. Mol Cancer 16: 9, 2017.
5. Bian Z, Jin L, Zhang J, Yin Y, Quan C, Hu Y, Feng Y, Liu H, Fei B, Mao Y, *et al*: LncRNA-UCA1 enhances cell proliferation and 5-fluorouracil resistance in colorectal cancer by inhibiting miR-204-5p. Sci Rep 6: 23892, 2016.
6. Siegel RL, Miller KD and Jemal A: Cancer statistics, 2017. CA Cancer J Clin 67: 7-30, 2017.
7. Wu X, Li R, Song Q, Zhang C, Jia R, Han Z, Zhou L, Sui H, Liu X, Zhu H, *et al*: JMJD2C promotes colorectal cancer metastasis via regulating histone methylation of MALAT1 promoter and enhancing beta-catenin signaling pathway. J Exp Clin Cancer Res 38: 435, 2019.
8. Gao P, Wang Z, Hu Z, Jiao X and Yao Y: Circular RNA circ_0074027 indicates a poor prognosis for NSCLC patients and modulates cell proliferation, apoptosis, and invasion via miR-185-3p mediated BRD4/MADD activation. J Cell Biochem 121: 2632-2642, 2020.
9. Feng Y, Yang Y, Zhao X, Fan Y, Zhou L, Rong J and Yu Y: Circular RNA circ0005276 promotes the proliferation and migration of prostate cancer cells by interacting with FUS to transcriptionally activate XIAP. Cell Death Dis 10: 792, 2019.
10. Li J, Yang J, Zhou P, Le Y, Zhou C, Wang S, Xu D, Lin HK and Gong Z: Circular RNAs in cancer: Novel insights into origins, properties, functions and implications. Am J Cancer Res 5: 472-480, 2015.
11. Hansen TB, Jensen TI, Clausen BH, Bramsen JB, Finsen B, Damgaard CK and Kjems J: Natural RNA circles function as efficient microRNA sponges. Nature 495: 384-388, 2013.
12. Cheng Z, Yu C, Cui S, Wang H, Jin H, Wang C, Li B, Qin M, Yang C, He J, *et al*: circTP63 functions as a ceRNA to promote lung squamous cell carcinoma progression by upregulating FOXM1. Nat Commun 10: 3200, 2019.
13. Song J, Wang HL, Song KH, Ding ZW, Wang HL, Ma XS, Lu FZ, Xia XL, Wang YW, Fei-Zou and Jiang JY: CircularRNA_104670 plays a critical role in intervertebral disc degeneration by functioning as a ceRNA. Exp Mol Med 50: 94, 2018.
14. Bai N, Peng E, Qiu X, Lyu N, Zhang Z, Tao Y, Li X and Wang Z: circFBLIM1 act as a ceRNA to promote hepatocellular cancer progression by sponging miR-346. J Exp Clin Cancer Res 37: 172, 2018.
15. Tong H, Zhao K, Wang J, Xu H and Xiao J: CircZNF609/miR-134-5p/BTG-2 axis regulates proliferation and migration of glioma cell. J Pharm Pharmacol 72: 68-75, 2020.
16. Chen Y, Li Z, Zhang M, Wang B, Ye J, Zhang Y, Tang D, Ma D, Jin W, Li X and Wang S: Circ-ASH2L promotes tumor progression by sponging miR-34a to regulate Notch1 in pancreatic ductal adenocarcinoma. J Exp Clin Cancer Res 38: 466, 2019.
17. Ren C, Zhang Z, Wang S, Zhu W, Zheng P and Wang W: Circular RNA hsa_circ_0001178 facilitates the invasion and metastasis of colorectal cancer through upregulating ZEB1 via sponging multiple miRNAs. Biol Chem 401: 487-496, 2020.
18. Li H, Jin X, Liu B, Zhang P, Chen W and Li Q: CircRNA CBL.11 suppresses cell proliferation by sponging miR-6778-5p in colorectal cancer. BMC Cancer 19: 826, 2019.
19. Du WW, Fang L, Yang W, Wu N, Awan FM, Yang Z and Yang BB: Induction of tumor apoptosis through a circular RNA enhancing Foxo3 activity. Cell Death Differ 24: 357-370, 2017.
20. Xing Y, Zha WJ, Li XM, Li H, Gao F, Ye T, Du WQ and Liu YC: Circular RNA circ-Foxo3 inhibits esophageal squamous cell cancer progression via the miR-23a/PTEN axis. J Cell Biochem 121: 2595-2605, 2020.
21. Xiao-Long M, Kun-Peng Z and Chun-Lin Z: Circular RNA circ_HIPK3 is down-regulated and suppresses cell proliferation, migration and invasion in osteosarcoma. J Cancer 9: 1856-1862, 2018.
22. Zhang H, Guo X, Feng X, Wang T, Hu Z, Que X, Tian Q, Zhu T, Guo G, Huang W and Li X: MiRNA-543 promotes osteosarcoma cell proliferation and glycolysis by partially suppressing PRMT9 and stabilizing HIF-1alpha protein. Oncotarget 8: 2342-2355, 2017.
23. Liu S, Song L, Zhang L, Zeng S and Gao F: miR-21 modulates resistance of HR-HPV positive cervical cancer cells to radiation through targeting LATS1. Biochem Biophys Res Commun 459: 679-685, 2015.
24. Livak KJ and Schmittgen TD: Analysis of relative gene expression data using real-time quantitative PCR and the 2(-Delta Delta C(T)) method. Methods 25: 402-408, 2001.
25. Kuo SJ, Liu SC, Huang YL, Tsai CH, Fong YC, Hsu HC and Tang CH: TGF-β1 enhances FOXO3 expression in human synovial fibroblasts by inhibiting miR-92a through AMPK and p38 pathways. Aging (Albany NY) 11: 4075-4089, 2019.
26. Dudekula DB, Panda AC, Grammatikakis I, De S, Abdelmohsen K and Gorospe M: CircInteractome: A web tool for exploring circular RNAs and their interacting proteins and microRNAs. RNA Biol 13: 34-42, 2016.
27. Betel D, Wilson M, Gabow A, Marks DS and Sander C: The microRNA.org resource: Targets and expression. Nucleic Acids Res 36 (Database issue): D149-D153, 2008.
28. Wang K, Long B, Liu F, Wang JX, Liu CY, Zhao B, Zhou LY, Sun T, Wang M, Yu T, *et al*: A circular RNA protects the heart from pathological hypertrophy and heart failure by targeting miR-223. Eur Heart J 37: 2602-2611, 2016.
29. Jin L, Han C, Zhai T, Zhang X, Chen C and Lian L: Circ_0030998 promotes tumor proliferation and angiogenesis by sponging miR-567 to regulate VEGFA in colorectal cancer. Res Square: Oct 20, 2020 (Epub ahead of print). doi: 10.21203/rs.3.rs-92165/v1
30. Meng S, Zhou H, Feng Z, Xu Z, Tang Y, Li P and Wu M: CircRNA: Functions and properties of a novel potential biomarker for cancer. Mol Cancer 16: 94, 2017.
31. Zhou J, Zhou LY, Tang X, Zhang J, Zhai LL, Yi YY, Yi J, Lin J, Qian J and Deng ZQ: Circ-Foxo3 is positively associated with the Foxo3 gene and leads to better prognosis of acute myeloid leukemia patients. BMC Cancer 19: 930, 2019.
32. Zhao H, Diao C, Wang X, Xie Y, Liu Y, Gao X, Han J and Li S: MiR-543 promotes migration, invasion and epithelial-mesenchymal transition of esophageal cancer cells by targeting phospholipase A2 group IVA. Cell Physiol Biochem 48: 1595-1604, 2018.
33. Liu X, Gan L and Zhang J: miR-543 inhibites cervical cancer growth and metastasis by targeting TRPM7. Chem Biol Interact 302: 83-92, 2019.
34. Liu G, Zhou J and Dong M: Down-regulation of miR-543 expression increases the sensitivity of colorectal cancer cells to 5-Fluorouracil through the PTEN/PI3K/AKT pathway. Biosci Rep 39: BSR20190249, 2019.
35. Xu J, Wang F, Wang X, He Z and Zhu X: miRNA-543 promotes cell migration and invasion by targeting SPOP in gastric cancer. OncoTargets Ther 11: 5075-5082, 2018.
36. Bartel DP: MicroRNAs: Target recognition and regulatory functions. Cell 136: 215-233, 2009.
37. Zhang J, Wang G, Chu SJ, Zhu JS, Zhang R, Lu WW, Xia LQ, Lu YM, Da W and Sun Q: Loss of large tumor suppressor 1 promotes growth and metastasis of gastric cancer cells through upregulation of the YAP signaling. Oncotarget 7: 16180-16193, 2016.
38. Furth N, Pateras IS, Rotkopf R, Vlachou V, Rivkin I, Schmitt I, Bakaev D, Gershoni A, Ainbinder E, Leshkowitz D, *et al*: LATS1 and LATS2 suppress breast cancer progression by maintaining cell identity and metabolic state. Life Sci Alliance 1: e201800171, 2018.
39. Deng J, Zhang W, Liu S, An H, Tan L and Ma L: LATS1 suppresses proliferation and invasion of cervical cancer. Mol Med Rep 15: 1654-1660, 2017.